TROUBLESHOOTING TURBOMACHINERY USING STARTUP AND COASTDOWN VIBRATION DATA

by

Ed Wilcox

Machinery Team Lead

Lyondell/Equistar

Channelview, Texas

Ed Wilcox is the Machinery Team Lead with Lyondell/Equistar, in Channelview, Texas. He is responsible for trobleshooting, repair, and condition monitoring of rotating equipment at both the Lyondell and Equistar facilities. Prior to this, Mr. Wilcox worked for more than 10 years with Conoco and Citgo as a Rotating Equipment Engineer. He has authored several papers in the areas of rotordynamics, vibration analysis, and performance testing.

Mr. Wilcox has a BSME degree from the University of Missouri-Rolla, and an MSME degree from Oklahoma State University. He has also done postgraduate work at the Georgia Institute of Technology in the areas of lubrication, rotordynamics, and vibration. He is a Vibration Institute Level III Vibration Specialist and a registered Professional Engineer in the State of Oklahoma.

ABSTRACT

Accurate and meaningful condition monitoring is necessary to prevent both severe equipment damage and unnecessary shutdowns. One of the most important aspects of condition monitoring is the evaluation of startup and shutdown vibration data. A considerable amount of upfront time must be committed to gather condition data when the machinery is known to be in good condition to provide an adequate picture of the current condition. Examples are given of problems that were correctly evaluated only through access and comparison to past startup/shutdown data as well as information obtained from a rotordynamic model of the system.

INTRODUCTION

This paper describes how transient vibration can be used to provide much more information about a piece of machinery than steady-state data alone. Transient vibration data are defined as vibration data taken when the machinery starts up or shuts down (i.e., large changes in speed). Most of the machinery described is of the high-speed nature with hydrodynamic journal bearings and noncontacting eddy current displacement probes, though many of the principles apply to low-speed applications with antifriction bearings. A brief description is given of the type of diagnostic equipment required to gather transient data. The different type of transient data plots are described along with the different insights they each provide. Likewise, several case studies are presented where transient data were used to evaluate the stability of the machinery as well as determine the source of the excitation forces. Another important benefit of transient data is that they provide a method of verifying machinery natural mode frequencies and rotordynamic models.

IMPORTANCE OF TRANSIENT DATA

Transient vibration provides a wealth of information that is not available from steady-state data. Among these are:

- The ability to compare the vibration amplitude, phase, shaft position, etc., at speeds above and below the shaft critical speeds
- The best signature of the overall rotor natural frequencies, which are normally a result of the complex relationship between the rotor supports (bearings, seals, etc.) and the dynamic nature of the rotor itself

Just as important as the comparisons listed above is the ability to compare transient data before and after a problem exists in the machinery. Assessments of machinery condition are made much easier when the ability to compare both before and after are available.

Likewise, it is very important to evaluate many different types of plots for displaying vibration data. Using only one type of plot limits the machinery specialist's ability to obtain an adequate "picture" of the machinery condition.

BASIC ROTORDYNAMICS

A basic understanding of rotordynamics is required to best interpret transient vibration data. A simplified model of a between-bearing rotor is provided by the Jeffcott rotor (Figure 1). The unbalanced disk is located in the center of the massless rotor on rigid supports. The only damping in the system is due to the viscous drag of the air. While the Jeffcott rotor is a very simple model, it can provide a wealth of insight into the effects of synchronous vibration in turbomachinery. An endview of the Jeffcott rotor shows the relationship between the center of mass (M) and the geometric center (C) (Figure 2). The synchronous phase angle (β) is the difference between the unbalance vector (U) and displacement vector (R). The amplitude of synchronous whirl and phase angle for the Jeffcott rotor as it passes through the rotor's first balance resonance (critical speed) is shown in Figure 3. The response amplitude equation is shown in Equation (1).

$$r = \frac{\omega^2 u}{\sqrt{\left(\frac{k}{m} - \omega^2\right)^2 + \left(\frac{c\omega}{m}\right)^2}} \tag{1}$$

A physical explanation of these graphs shows that well below the critical speed, the response vector R and unbalance vector U are in phase (i.e., $\beta \sim 0$). As the rotation speed is increased, the unbalance vector U begins to lead R. As the critical speed is transversed, β passes through 90 degrees, then asymptotically approaches 180 degrees at speeds above the critical. Thus at super-critical speeds, the rotor center of mass (M) moves to the center of the whirl orbit and stands still, while the shaft center whirls around the center of mass. Additionally, the effect nonfrequency dependent forces have on the whirl amplitude is shown in Figure 4. The actual synchronous response will be some combination of Figures 3 and 4.

An illustration of the spring, damping, and unbalance forces is shown in Figure 5 for the Jeffcott rotor at speeds below, at, and above the first balance resonance. As can be seen, far below the

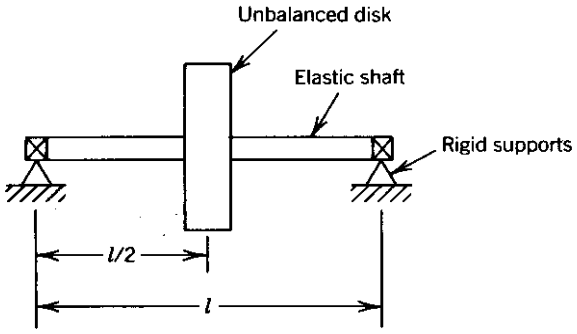

Figure 1. The Jeffcott Rotor. (Courtesy Vance, 1988)

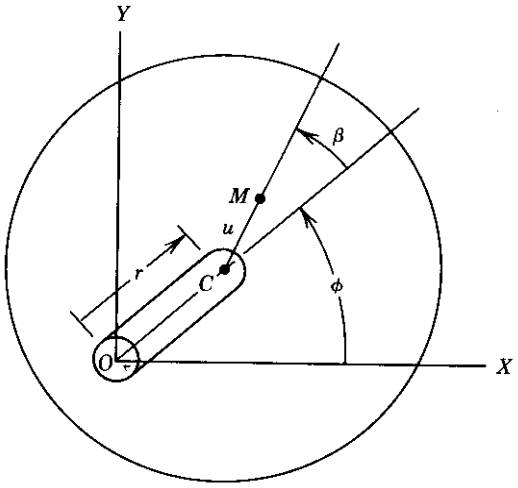

Figure 2. End View of the Jeffcott Rotor. (Courtesy Vance, 1988)

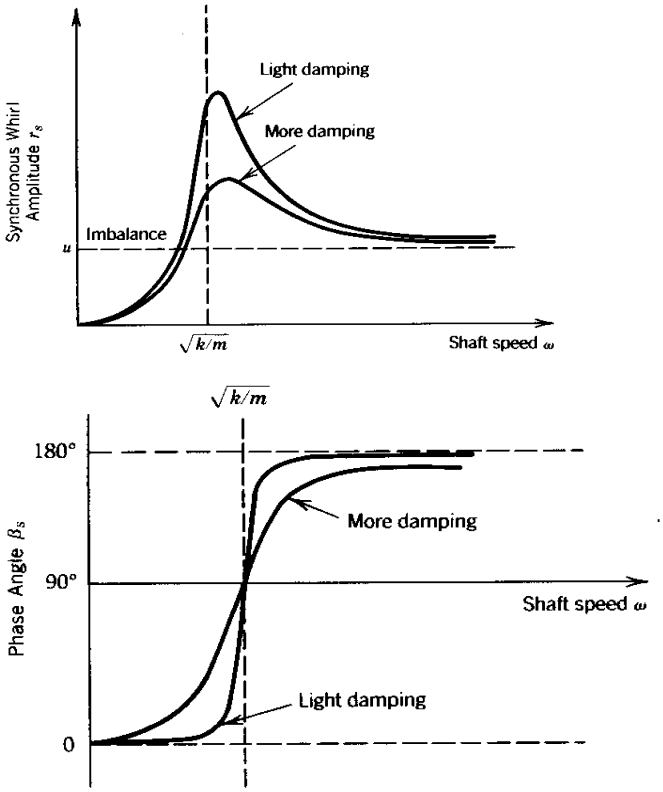

Figure 3. Synchronous Response and Phase Angle of the Jeffcott Rotor. (Courtesy Vance, 1988)

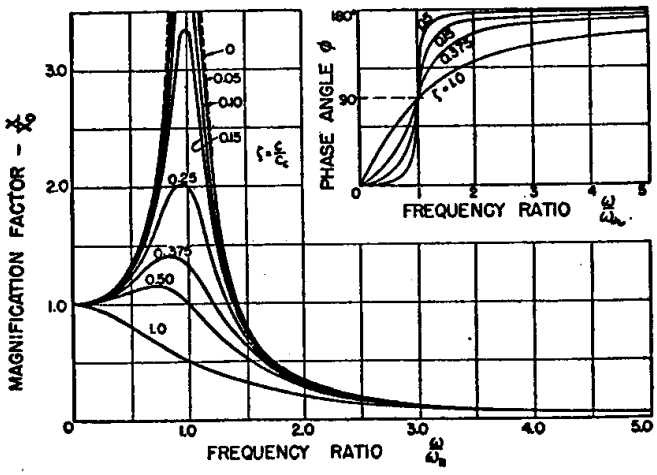

Figure 4. Synchronous Response to Constant Force, I.E., Misalignment. (Courtesy Vance, 1988)

first balance resonance, the shaft stiffness is approximately equal to the unbalance force. However, at resonance, the damping is the only term that restricts the displacement due to unbalance. Likewise, as the speed increases past the resonance, the whirl amplitude, *r*, approaches the value of the center of mass eccentricity, *u* (assuming there are no other excitation forces such as misalignment, internal friction, etc.).

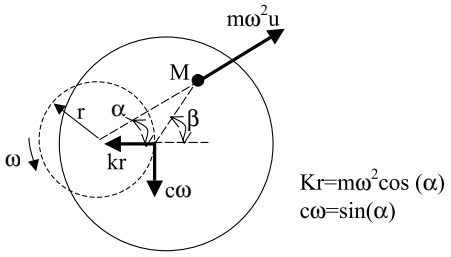

$\omega << \omega_n$	$\alpha \sim 0$ $\beta \sim 0$	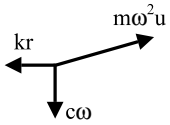	$Kr \sim m\omega^2 u$
$\omega = \omega_n$	$\alpha \sim \pi/2$ $\beta \sim \pi/2$	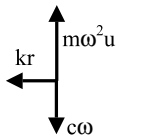	$c\omega \sim m\omega^2 u$
$\omega >> \omega_n$	$\alpha \sim \pi$ $\beta \sim \pi$	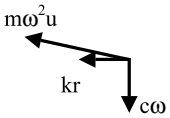	$r \rightarrow u$

Figure 5. Synchronous Response Below, At, and Above the Critical Speed.

Since at resonance, the damping is the only force that contains the Jeffcott rotor displacement, measuring displacement as the rotor passes through resonance is a good method to determine the

amount of damping in the rotor system. The synchronous amplification factor (Q) is a measure of the severity of a resonance, as well as an indication of the damping present. While there are several methods available to measure Q, the half power method is used here because it is the most widely accepted. The basic definition is given below in Equation (2).

$$Q = \frac{\text{Resonance Frequency}}{\text{Frequency bandwidth @} - 3dB} = \frac{N_{cr}}{N_2 - N_1} \tag{2}$$

The frequency bandwidth is the difference between the frequencies where the amplitude is 3 dB below the maximum at peak resonance. This corresponds to 0.707 times the amplitude at resonance. This method has been adopted by the American Petroleum Institute (API) for measuring the synchronous amplification factor (Figure 6).

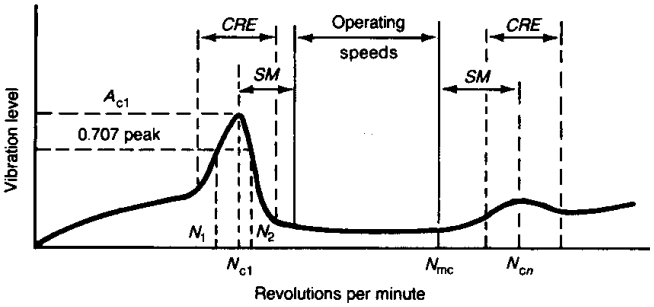

N_{c1} = Rotor first critical, center frequency, cycles per minute.
N_{cn} = Critical speed, nth.
N_{mc} = Maximum continuous speed, 105 percent.
N_1 = Initial (lesser) speed at 0.707 × peak amplitude (critical).
N_2 = Final (greater) speed at 0.707 × peak amplitude (critical).
$N_2 - N_1$ = Peak width at the half-power point.
AF = Amplification factor
$= \frac{N_{c1}}{N_2 - N_1}$
SM = Separation margin.
CRE = Critical response envelope.
A_{c1} = Amplitude at N_{c1}.
A_{cn} = Amplitude at N_{cn}.

Figure 6. API Definition of Synchronous Amplification Factor.

Generally, machines with synchronous amplification factors below four are considered to be very well damped. Values between four and eight are considered adequately damped and are normally stable. Between eight and 15 are considered marginal, though many older machines may operate in the area. Amplification factors above 15 are considered to have insufficient damping and are very likely to experience rubs on startup and stability problems.

The synchronous amplification factor is an important diagnostic parameter for evaluating the stability of the machinery and comparing the machinery condition before and after a problem exists with the equipment. As can be seen in Figure 3, the amplification factor increases as the system damping decreases. Since most of the damping in high-speed machinery comes from the hydrodynamic bearings, changes in the synchronous amplification factor can indicate a change in the damping provided by the bearings. Which in turn can indicate a change in the condition of the bearings.

Since most turbomachinery is supported on hydrodynamic bearings, the effects of flexible supports need to be considered as well. The Jeffcott rotor can be modified to have flexible bearing supports (Figure 7). Flexible supports are very desirable from a rotordynamics standpoint because they:

- May reduce the dynamic load transmitted to the casing.
- Allow the damping in the bearings to be more effective (i.e., softer bearings allow more velocity at the bearings, which is required for damping).

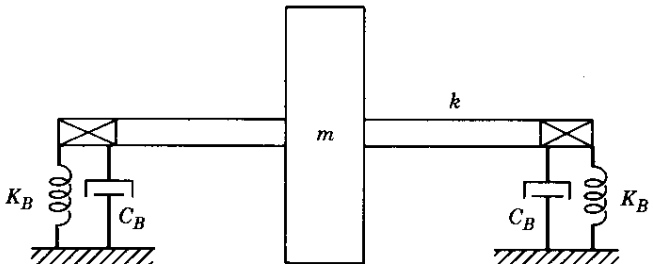

Figure 7. Jeffoctt Rotor with Flexible Supports. (Courtesy Vance, 1988)

The calculated transmissibility ratio (F_B/F_∞) for different values of damping is shown in Figure 8. As can be seen, the damping lowers the force transmitted to the bearings at resonance, but actually causes it to be higher for $\omega/\omega_n > 1.14$. This is in contrast to Figure 3, where damping has a desirable effect on whirl amplitude for the entire speed range. Generally speaking, it is desirable (from a synchronous response and stability viewpoint) for the bearing to shaft stiffness ratio (K_B/K_{shaft}) to be as low as possible, with the obvious restriction that the low bearing stiffness should not cause the machine to operate closer to a balance resonance (Barrett, et al., 1978).

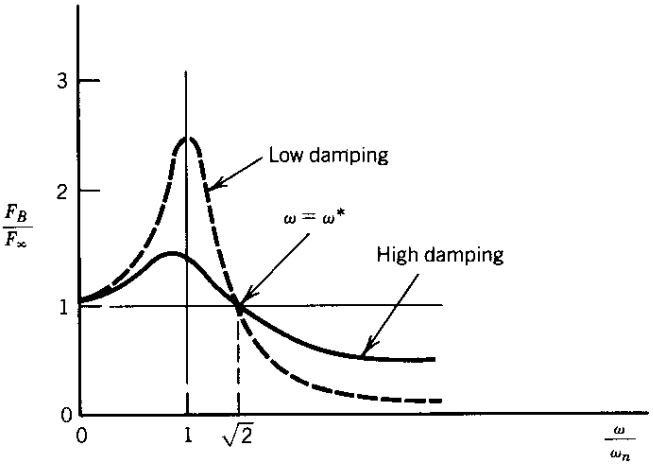

Figure 8. Transmissibility Versus Shaft Speed Ratio. (Courtesy Vance, 1988)

Furthermore, rotor support stiffness is not always in the principal direction (i.e., principal stiffnesses produce a force opposite in direction to the rotor displacement). The stiffness and damping coefficients of a bearing or seal support can be divided into the following (Figure 9). The K_{xy} and K_{yx} terms are commonly called "cross-coupled" terms (if the shaft is displaced in the vertical direction, the cross-coupled stiffness produces a reaction force in the horizontal direction) and reduces the positive effects of damping if K_{xy} $(-K_{yx}) > 0$. For this reason, when $K_{xy} > 0$, the amplification factor of the rotor is increased and the stability is reduced. Equation (3) gives the response of a rigid rotor on flexible supports, including cross-coupled effects. Note that when $K_{xy} > 0$, it reduces the damping term and increases the amplification factor. For this reason, when the amplification factor is measured from field data, it is actually a measure of the combination of direct damping and cross-coupled stiffness present in the machine.

$$r = \frac{\omega^2 u}{\sqrt{\left(\frac{2k}{m} - \omega^2\right)^2 + \left(\frac{2c\omega}{m} - k_{xy}\right)^2}} \tag{3}$$

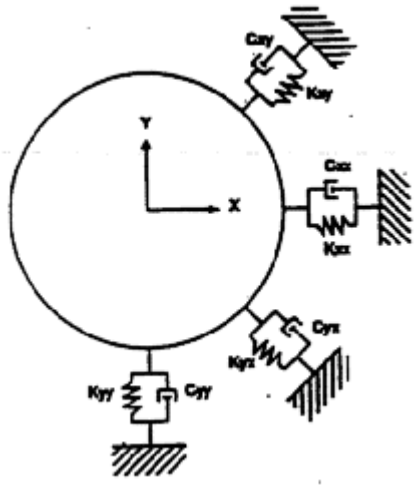

Figure 9. Support Coefficients. (Courtesy Bielk and Leader, 1994)

DIAGNOSTIC EQUIPMENT

Obtaining startup/shutdown vibration data require somewhat specialized diagnostic equipment. While many handheld vibration analyzers today have the ability to take startup/shutdown data, they are normally limited to one or two channels with limited plot capabilities. For a piece of high-speed turbomachinery, with noncontacting shaft displacement probes, a system similar to Figure 10 is required to obtain adequate startup/shutdown vibration data. While many people today will not include the tape recorder, it should be understood that the digital systems today do not record the raw vibration signal, only certain digitized elements. The tape recorder provides a copy of the vibration data that can be used for analysis repeatedly. Often times when the digital system is used by itself, the operator may inadvertently make an error on the acquisition parameters. For example, maybe the maximum speed for the keyphasor is set too low or the trigger between shaft speeds is too low or too high. If the digital system is used by itself, important data may be lost and may not be obtainable because the machinery cannot be shut down or started up again or, worse, because it was damaged. One way to improve the reliability of the data acquisition process is to simulate the machinery shutdown or startup prior to the actual event. This can be accomplished with a rotor kit (Figure 11). The rotor kit can usually be adjusted to have similar acceleration/deceleration times as the machine in question. This allows the machinery specialist to review the data provided by the diagnostic equipment prior to the actual machinery event and make sure that all the data required are recorded.

The following concerns should be addressed before the data acquisition process begins:

• *Number of samples*—While the analog tape record has somewhat unlimited recording space, the newer digital systems do not. Most digital systems have a limited number of vector and waveform samples that can be recorded before the data have to be written to the hard-drive of the computer. When this happens, data acquisition stops, while the data is being written to the hard-drive. For this reason, the sampling method (i.e., delta speed or delta time) must be adjusted based on the machinery configuration to ensure that enough data are taken for analysis, but not so much that the maximum samples are exceeded.

• *Max frequency/number of lines*—Depending upon the machinery configuration and the purpose of the analysis, the maximum frequency and number of lines for the fast Fourier transform (FFT) algorithm become very important. On machinery that is driven by electric motors, the acceleration time is many times quite rapid (i.e., less than 10 seconds). For these applications, to get adequate data the maximum frequency should be as high as reasonable to reduce the time for data acquisition. Similarly, the number of lines should be as low as possible while still providing adequate resolution. If the specialist is interested mostly in synchronous vibration, the resolution will not be as important as the number of samples obtained. However, if multiple nonsynchronous frequencies are present in the vibration signal, the resolution obviously becomes more important.

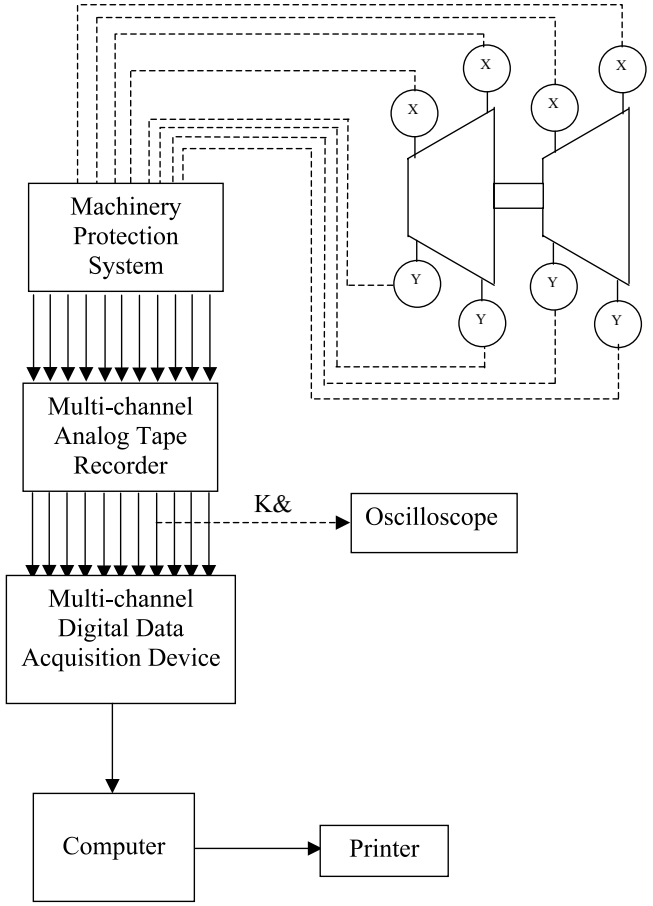

Figure 10. Diagnostic Equipment Required for Startup/Shutdown Data.

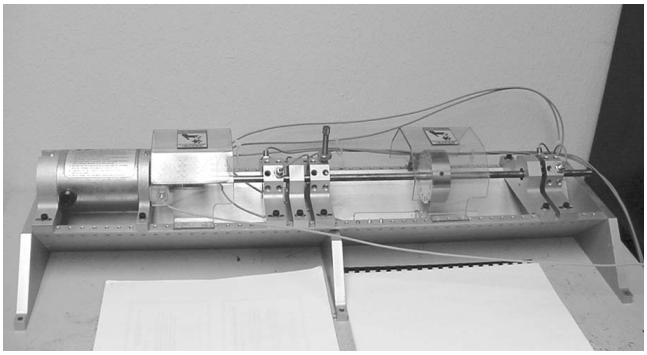

Figure 11. Rotor Kit.

• *Number of vectors per waveform sample*—Some digital systems do not record a waveform sample for every vector sample (to save memory and increase sample speed). For this reason, the sample frequency should be closely examined to give the correct number of spectra (i.e., more vector samples may be required than are necessary to obtain adequate waveform samples).

• *Keyphasor voltage*—The keyphasor signal is extremely important, since most of the digital analysis is dependent upon this

value. For this reason, the voltage change produced by the keyphasor should be set up correctly in the software and monitored during the data acquisition using the oscilloscope shown in Figure 10.

As can be seen, the digital systems require a large amount of input from the specialist to obtain meaningful data. For this reason, the tape backup becomes even more important on critical unspared machinery.

TYPES OF TRANSIENT DATA PLOTS

Transient vibration data can be displayed in many different formats. Each different type can reveal information that is not readily available from the other. For this reason, all the types should be used when evaluating the condition of a machine. The different types of plot are:

- Bodé/polar
- Cascade/waterfall
- Shaft centerline
- Orbit

This paper gives a description of each type of plot along with what can be determined from it.

Bodé and Polar Plots

Bodé plots are the most common method of displaying transient data. They normally display overall or synchronous vibration (however, nX data can be displayed as well) and corresponding phase, versus speed (Figure 12). The rotor natural frequencies can be determined by locating the peak in the vibration amplitude that corresponds to a phase shift of approximately 180 degrees.

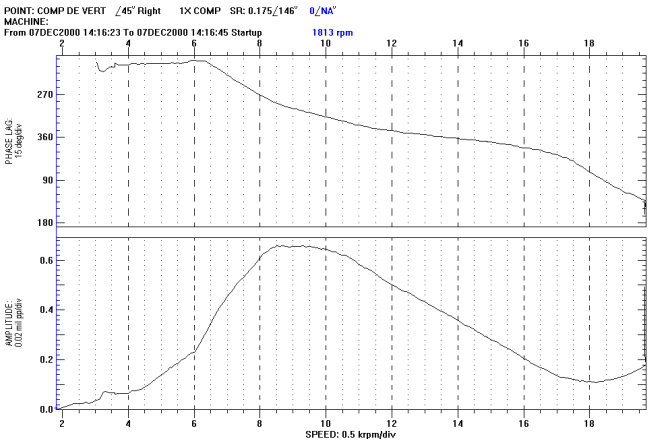

Figure 12. Bodé Plot.

Polar plots show the same data as Bodé plots, just in a different format (Figure 13). Sometimes, polar plots make it easier to determine when the rotor has transversed its critical speed, because the phase change is obvious (i.e., every 180 degrees on the plot). For example, from the Bodé plot shown in Figure 12 it is not immediately obvious that this rotor is approaching its second critical. However, one look at the polar plot in Figure 13, and it is very clear.

For the most accurate Bodé or polar plot, the vector data must be runout compensated. All probe areas have a certain amount of physical and/or electrical runout. The vector data are corrected for this runout by vectorally subtracting the vibration vector at a very low rpm from all the vector data obtained. Figures 14 and 15 show both the compensated (dashed) and uncompensated (solid) vector data. As can be seen, the compensated data show the vibration goes to zero.

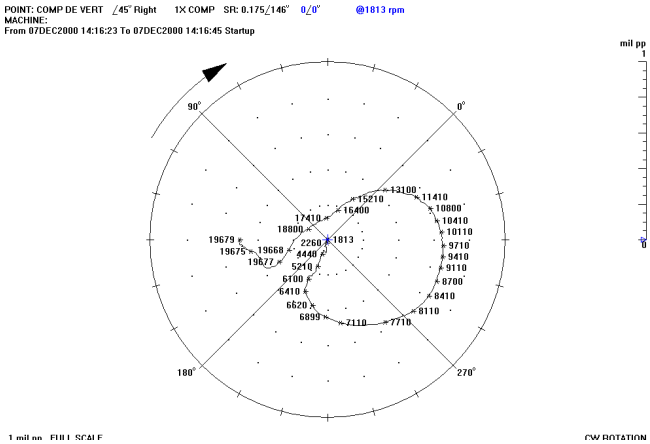

Figure 13. Polar Plot of Centrifugal Compressor Drive-End Bearing.

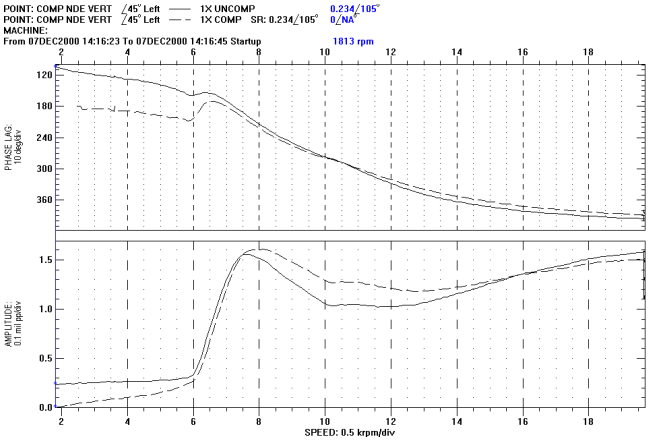

Figure 14. Bodé Plot Showing Compensated and Uncompensated Data.

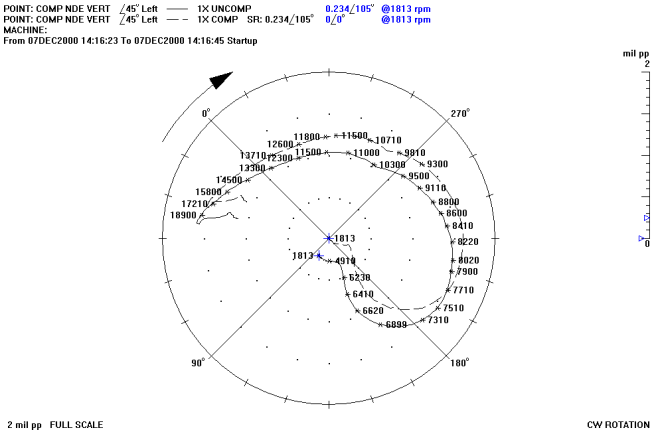

Figure 15. Polar Plot Showing Compensated and Uncompensated Data.

Case Study 1—Centrifugal Compressor with Increasing Radial Synchronous Vibration after Some Shutdowns

A particular high-speed centrifugal compressor was experiencing large increases in synchronous radial vibration after some (but not all) shutdowns (Figure 16). Likewise, it was noticed that the increase in vibration only occurred when the compressor tripped, not when it was intentionally shut down by operations. Normally, increases in synchronous radial vibration are caused by

either increased unbalance or bearing clearance. A natural assumption was that the bearings were being damaged somehow during coastdown. However, the bearing temperatures were normal (i.e., < 180°F). Likewise, both lube oil pumps, as well as the lube oil rundown tank, were functioning properly. Additionally, the probe gap voltages had not increased, indicating that the rotor had not dropped down in the bearings.

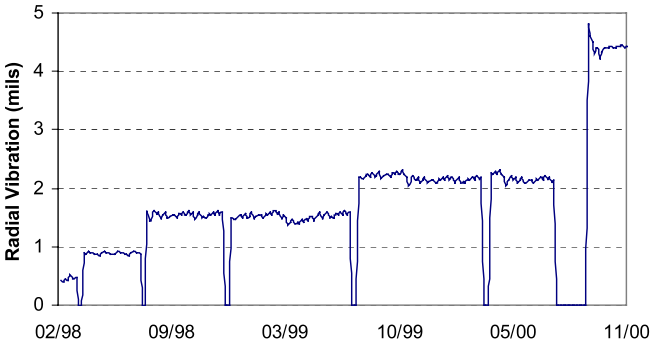

Figure 16. Increase in Radial Vibration after Compressor Trips over Time.

Records of the transient vibration data from the mechanical test from the original equipment manufacturer (OEM) were found showing the shaft radial vibration during startup (Figure 17). Additionally, transient data were recorded during several of the compressor shutdowns (Figures 18 and 19). Although the synchronous radial vibration had increased from 0.4 mils to 4.0 mils (i.e., Figure 19), the measured amplification factor had remained approximately the same (~ 4 to 5). This indicated that the damping produced by the bearings was the same, which meant that unbalance was probably the source of the problem. At the next available opportunity, the compressor bearings were inspected and found to be in excellent condition. The rotor was pulled and found to be heavily fouled with an oil catalyst residue. The bearings were reused and the rotor cleaned. The vibration dropped to approximately 0.5 mils with the clean rotor. Additionally, it was determined that if the compressor tripped, process gas that contained oil would leak back through the discharge check valve into the compressor, which was causing the fouling. If the compressor was shut down normally, a control valve was closed that prevented gas from backing into the compressor. Knowing that the source of vibration was probably deposits on the rotor allowed maintenance to be prepared for a rotor changeout (i.e., spare rotor prepared, rigging available, additional crews), which reduced both maintenance costs and operational downtime.

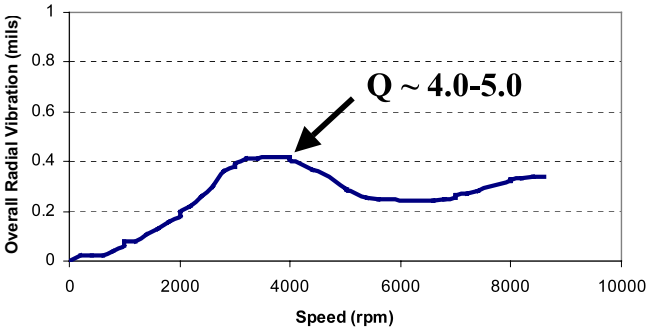

Figure 17. Transient Data from Mechanical Test at OEM Facility.

Case Study 2—Centrifugal Compressor with High Radial Synchronous Vibration after Previous Shutdown

A high-speed barrel compressor tripped due to an instrumentation failure. After the compressor was restarted, the nondrive-end (NDE) radial vibration increased from approximately 0.5 to 2.0

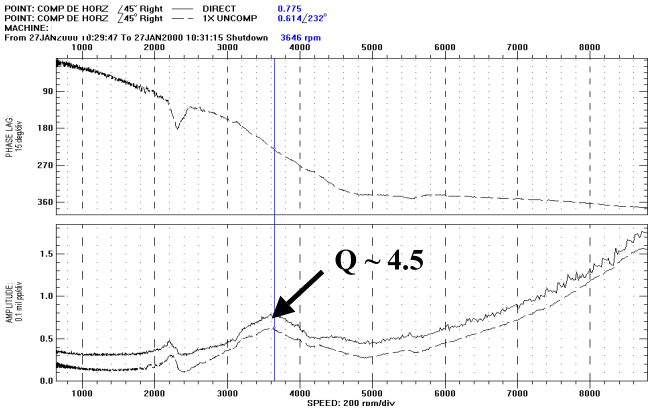

Figure 18. Transient Data after Two or Three Trips.

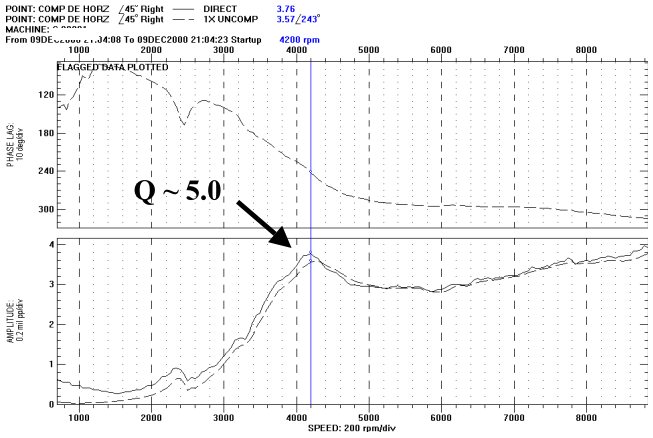

Figure 19. Transient Data from Last Startup, Shortly before Overhaul.

mils. All the vibration was synchronous. As in the previous case study, it was assumed that the bearings had been damaged during coastdown. The bearing damage was verified when transient data recorded during a planned shutdown (approximately one year after the instrumentation failure) were compared to transient data from a shutdown prior to the instrumentation failure (Figures 20 and 21).

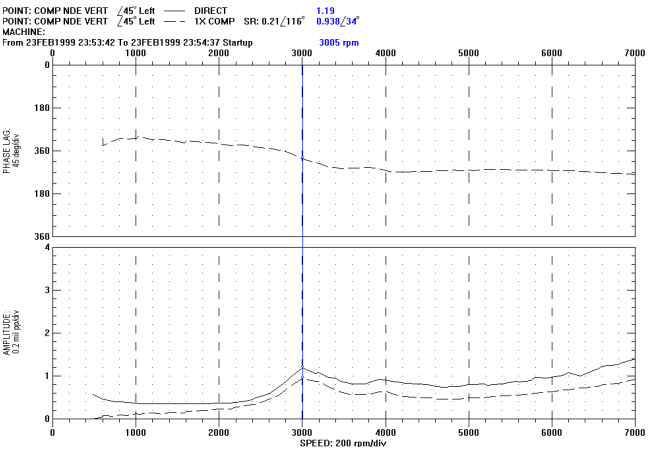

Figure 20. NDE Vertical Vibration Prior to Instrumentation Trip.

As can be seen, the amplification factor on the NDE bearing had increased dramatically. Inspection of the NDE bearing found that the lower pads were indeed wiped (Figure 22). After the NDE bearing was replaced, the compressor vibration returned to normal (Figure 23).

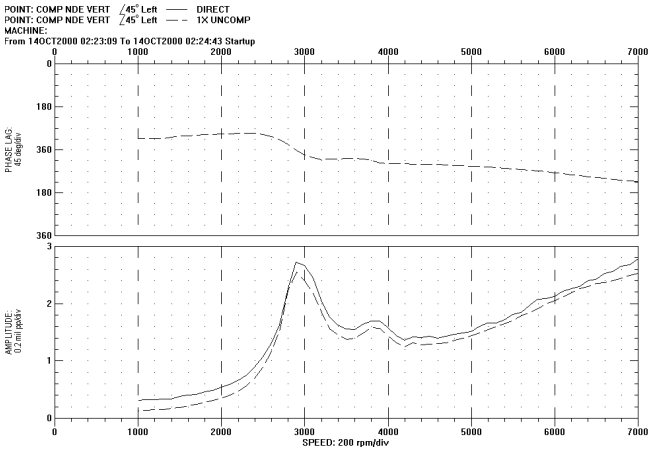

Figure 21. NDE Vertical Vibration after Bearing Damage.

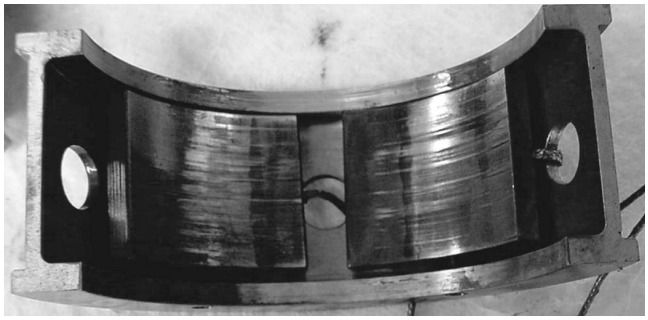

Figure 22. Lower Half of NDE Tilt-Pad Bearing.

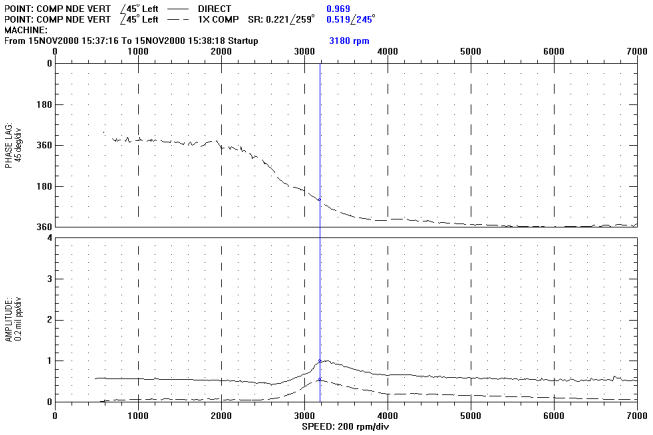

Figure 23. NDE Vertical Vibration after Bearing Replacement.

Case Study 3—Centrifugal Compressor with High Synchronous Vibration

A centrifugal compressor experienced a large increase in synchronous radial vibration, mostly on the inboard end (3 to 4 mils) and was shut down to inspect the bearings. The excessively high vibration had severely damaged the radial bearings (Figure 24) as well as the bearing housing itself. Due to business constraints, the bearings/housings were replaced/repaired and the compressor was restarted, although the cause of the high vibration was unknown. On startup, it was observed that the measured first critical speed had increased from approximately 4500 cpm to 6800 cpm (Figure 25). Since the thrust load had increased, this seemed to indicate that the rotating labyrinth on the balance piston might be rubbing the abraidable stationary, which would raise the first critical by effectively decreasing the bearing span. The radial vibration stayed at high, but acceptable, levels for three months until the compressor was shut down for a scheduled unit outage. A rub was found in the machine, but not at the balance piston seal. One of the diaphragms had broken and was being forced forward against the rotor (Figures 26 and 27). The diaphragm was repaired and the measured first critical returned to normal (Figure 28).

Figure 24. Damaged Radial Bearing.

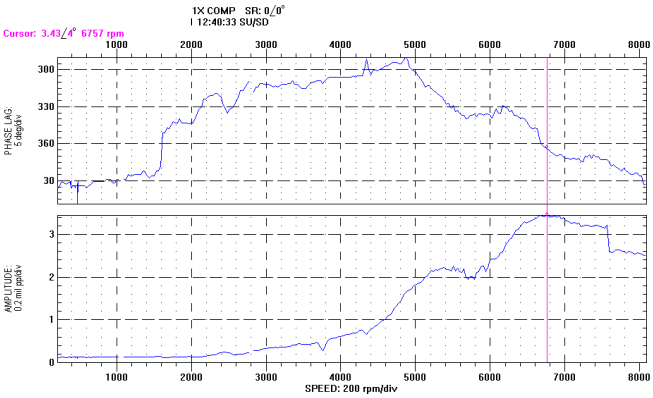

Figure 25. Startup Showing Abnormally High First Critical.

Figure 26. Damaged Inlet Guide Vanes/Diaphragms.

Cascade/Waterfall Plots

Cascade/waterfall plots are simply fast Fourier transforms at different speeds on the same plot. They are used to diagnose

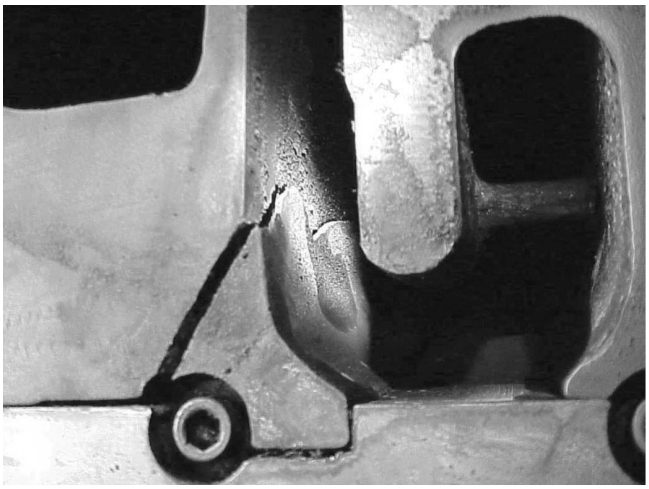

Figure 27. Cracked Diaphragm.

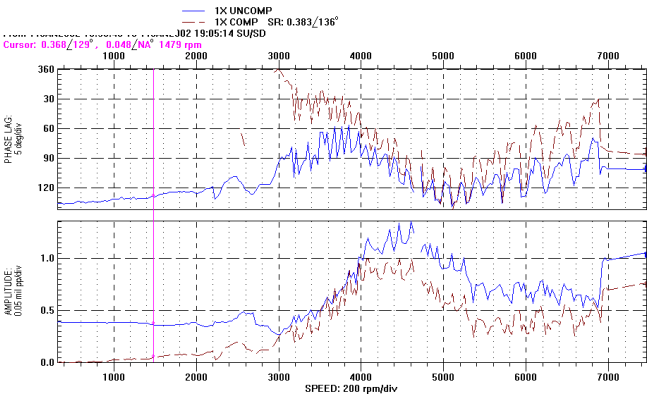

Figure 28. Bodé Plot after Overhaul.

nonsynchronous vibration problems that may appear (and disappear) at different rotational speeds. One of the most common problems diagnosed with these plots is oil "whirl" that turns into oil "whip." An illustration and example of this are given in Figures 29 and 30. As can be seen, the subsynchronous vibration tracks with the shaft speed until it coincides with the first natural mode of the machine. At this point, it "locks" onto this frequency regardless of the change in rotational speed. This is the point when oil "whirl" turns into oil "whip." In contrast, Figure 31 shows a centrifugal compressor that is experiencing rotating stall due to a large drop in the molecular weight of the process gas. As can be seen, at design speed (8000 rpm), the rotating stall is exciting the first natural mode of the compressor at 2700 cpm. As the compressor shuts down, the subsynchronous vibration drops away. A different compressor had been experiencing erratic subsynchronous vibration. A rotordynamic analysis of the compressor reveals that if the oil seal rings locked up, the first natural mode became unstable. This was verified, during a startup of the compressor, when the first mode was excited (Figure 32). As can be seen, the subsynchronous vibration appears, then drops away as the compressor starts up.

SHAFT CENTERLINE PLOTS

Shaft centerline plots show the location of the journal center, relative to the proximity probes. This type of data is only available when using proximity probes because the actual shaft location is determined from the DC component of the vibration signal, which gives the actual distance from the probe tip to the shaft (i.e., not the vibration). This information is most useful to the machinery specialist if it is recorded over time, especially as the speed

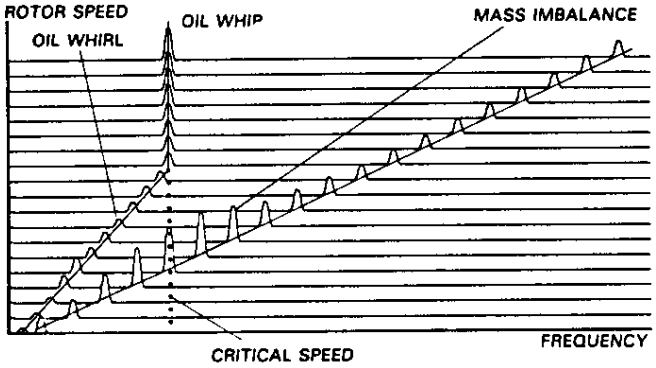

Figure 29. Illustration Showing Transition from Oil "Whirl" to Oil "Whip." (Courtesy Vance, 1988)

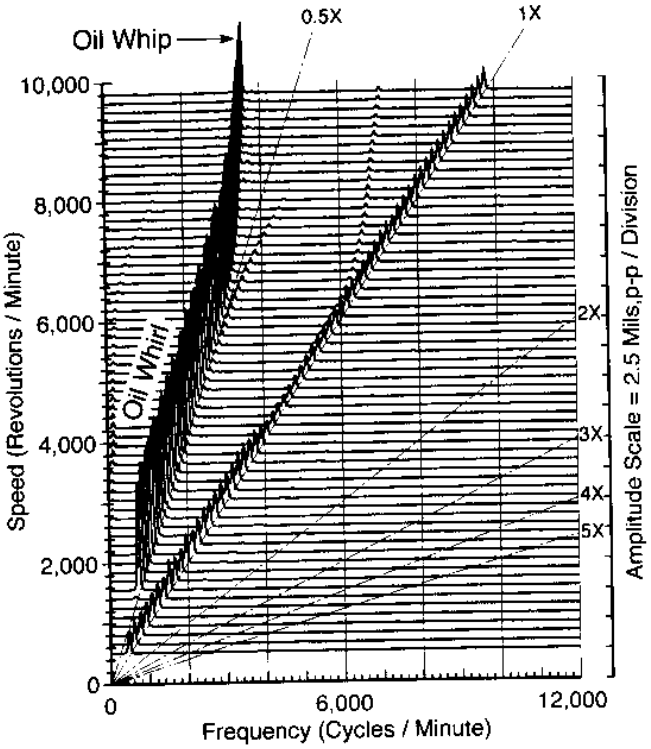

Figure 30. Cascade Plot Showing Transition from Oil "Whirl to Oil "Whip." (Courtesy Eisenmann and Eisenmann, 1998)

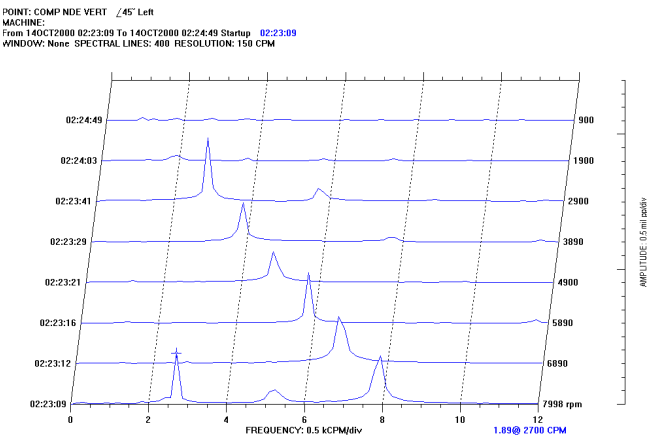

Figure 31. Centrifugal Compressor with Rotating Stall/Surge that Excites the First Mode.

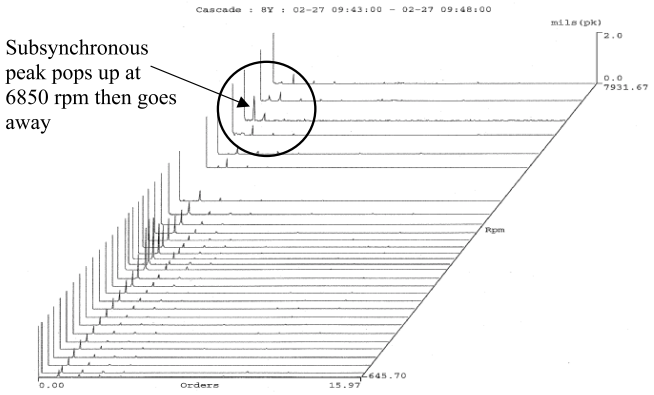

Figure 32. Waterfall Plot Showing Subsynchronous Vibration Appear, Then Disappear.

changes (i.e., absolute values by themselves are meaningless). Shaft centerline plots over long periods of time (i.e., months/years) can also provide insight into the degradation of a bearing. A journal develops an oil wedge between it and the bearing at a very low rotational speed (dependent upon the journal load and bearing configuration) (Figure 33). This causes the journal to rise in the bearing when the machinery begins to rotate. As the speed continues to increase, the journal typically continues to rise in the bearing, as the pressure developed by the hydrodynamic action of the wedge increases.

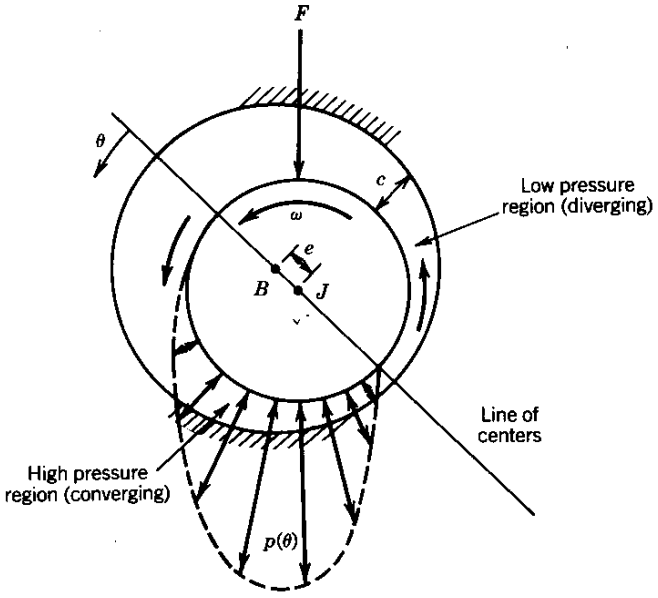

Figure 33. Oil Wedge Developed by Hydrodynamic Bearings. (Courtesy Zeidan, 1991, Turbomachinery Laboratory)

Case Study 4—Centrifugal Compressor with Excessive Radial Bearing Temperature

The drive-end radial bearing temperature of a high-speed centrifugal compressor was excessive after overhaul. The temperature would spike up rapidly to 300+°F (150°C) if it rained on the compressor (Figure 34). The bearing clearance was quite low (0.0045 inch on a 3.5 inch journal at 11,500 rpm), and it was decided that the bearing housing was contracting on the bearing during the rainstorm and reducing the clearance further. The compressor was shut down to install another bearing with higher clearance. The shaft centerline plots of the drive-end (DE) and NDE bearings are shown in Figures 35 and 36 during the coastdown. As can be seen, the drive-end journal did not drop at all as the machine coasted down from approximately 11,000 rpm. Examination of the bearings on the DE of the compressor revealed that the clearance was much too tight (Figure 37). Obviously, the top pads on this type of machine should not show evidence of wear. Bodé plots for this machine did not indicate a problem (Figure 38). This type of problem was only evident from the shaft centerline plots. After a bearing with more clearance was installed, the shaft centerline plot appears normal for the drive-end bearing on startup (Figure 39).

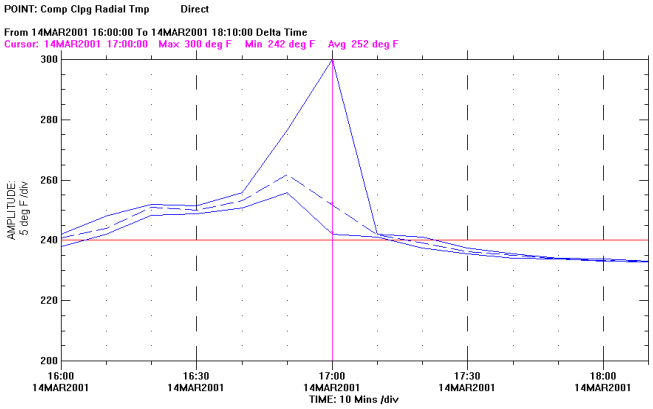

Figure 34. Radial Bearing Temperature Spike During Rainstorm on Centrifugal Compressor.

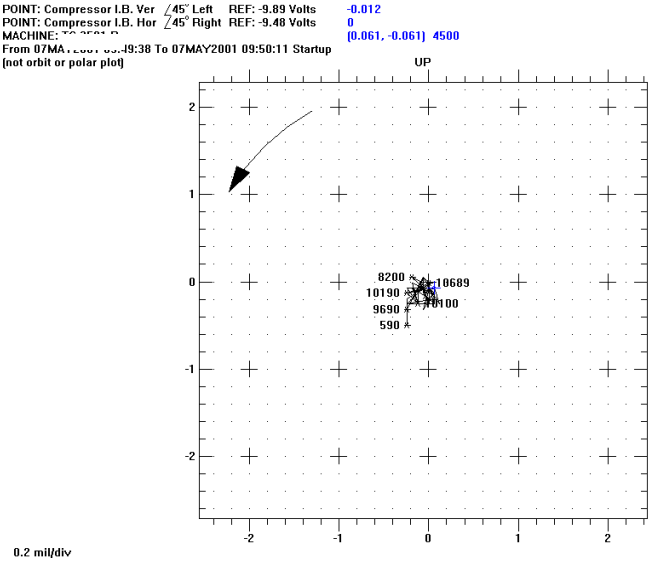

Figure 35. Shaft Centerline Plot of Compressor DE Bearing with Inadequate Clearance.

Case Study 5—Centrifugal Compressor with Excessive Radial Bearing Temperature

In a similar problem to the previous case study, a centrifugal compressor was overhauled and the radial bearing temperature on the nondrive-end was high (~ 240°F) after startup. At the time, it appeared to be a bad resistance temperature detector (RTD) because the wires had been cut and spliced during installation. Over the next year, the temperature slowly crept up until it reached 275°F. The temperature was controlled at or below 275°F by adding additional cooling to the lube system. The vibration technician reported that the gap voltage from the shaft displacement probes was increasing (Figure 40). This seemed to indicate that the journal was dropping down in the bearing. Closer examination of the gap voltage graph reveals that the voltage is becoming less negative (i.e. the journal

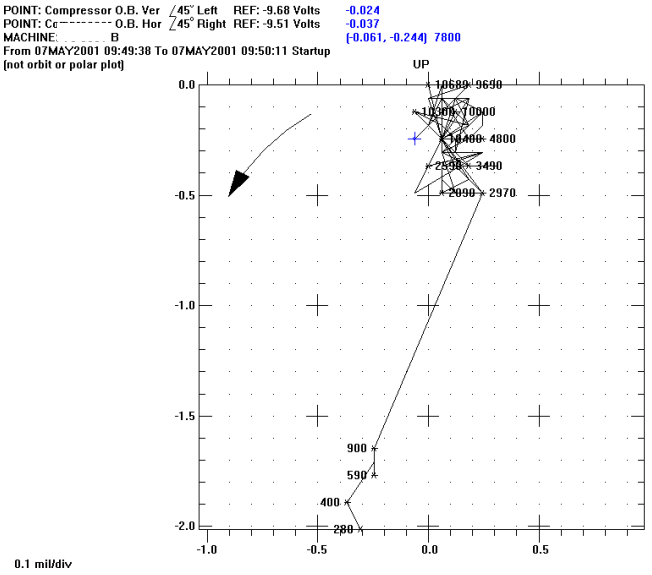

Figure 36. Shaft Centerline Plot of NDE Bearing.

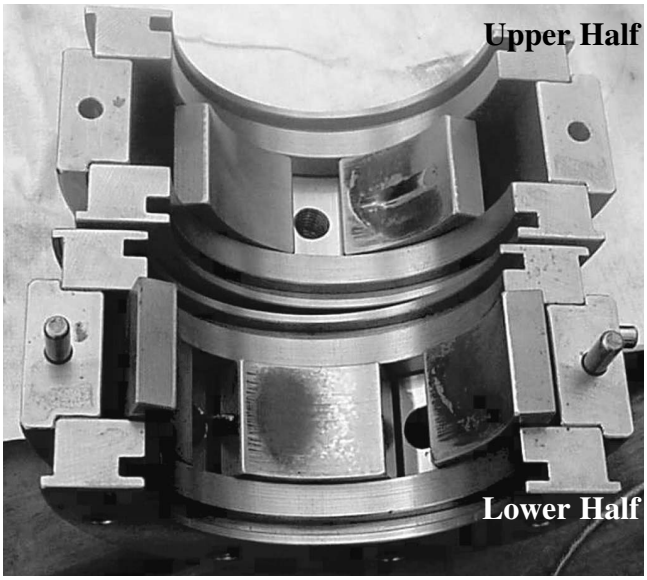

Figure 37. Damaged Bearing Showing Affects of Inadequate Clearance.

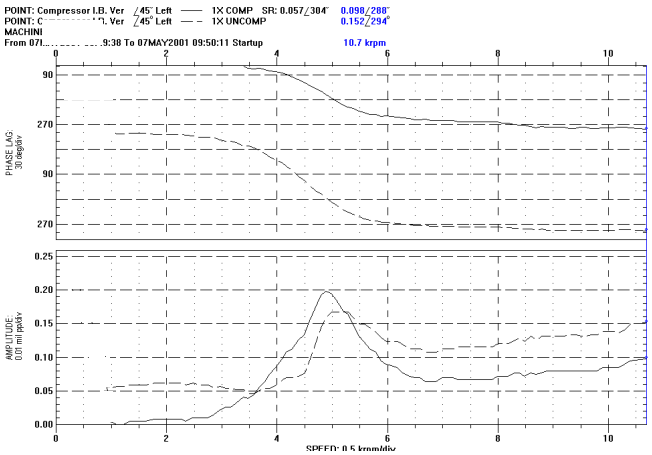

Figure 38. Bodé Plot.

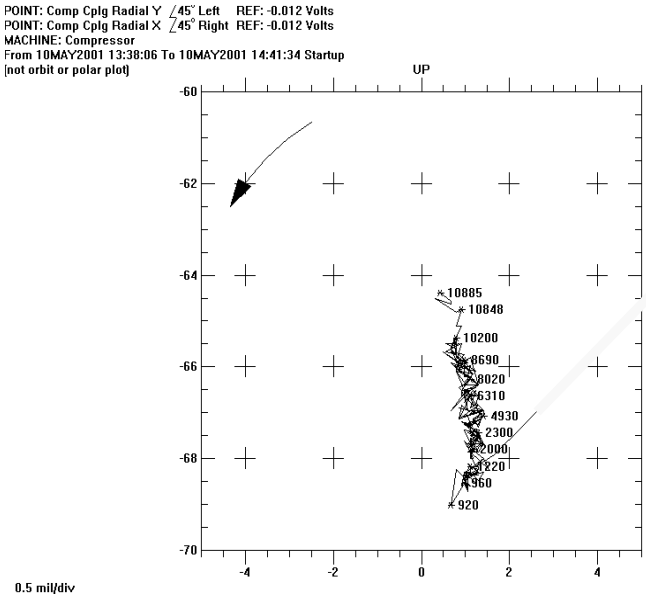

Figure 39. Shaft Centerline Plot of DE Journal with Proper Bearing Clearance.

is rising in the bearing, getting closer to the probes). This is the opposite direction that would be expected if the pads were wiping. Approximately one month later, the radial vibration on the NDE temporarily spiked up from 0.5 to 2.0 mils. Since a spare rotor was not available for this compressor, it was decided to shut down the compressor immediately and inspect the bearings (Figure 41). Note that the amplification factor is relatively low. Inspection of the bearing after the compressor was shut down revealed a heavy varnish on the pads (Figure 42). Furthermore, the babbitt had fatigued above the RTD on one of the lower pads as well (Figure 43). Close inspection of the bearing and bearing housing revealed that the porting from the bearing housing to the bearing did not line up, which was restricting the lube oil flow to the bearing. It was remarkable that the bearing received any oil at all. The porting was corrected and the compressor was started with no problems. The measured Bodé plot on startup was unchanged from what was seen on shutdown (Figure 44). This was expected since the bearing had not been damaged yet.

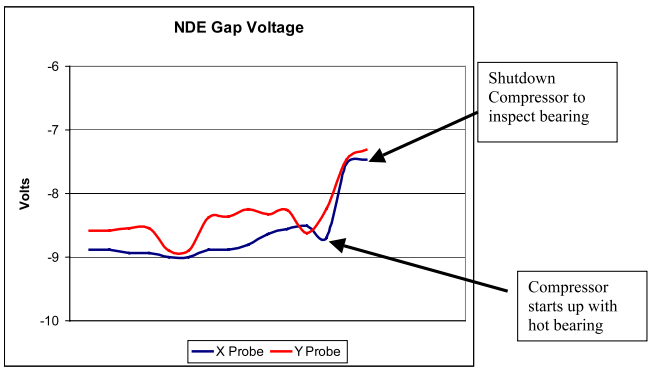

Figure 40. Gap Voltage of NDE Probes.

ORBIT PLOTS

An orbit shows the displacement of the journal inside the bearing clearance. Figure 45 shows a 1× filtered orbit (that is why it is so smooth). To view the nonsynchronous shaft vibration requires examining the unfiltered orbit (Figure 46). Orbits are normally steady-state plots (not actually steady-state, just at one speed). However, orbits at different speeds can be compared to

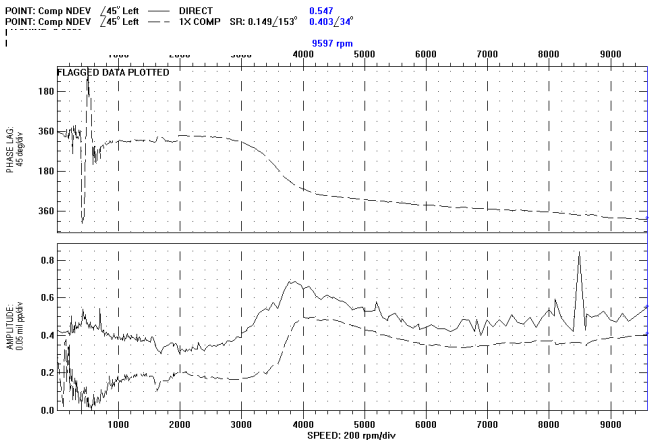

Figure 41. Shutdown Bodé Plot of Centrifugal Compressor with High NDE Radial Bearing Temperature.

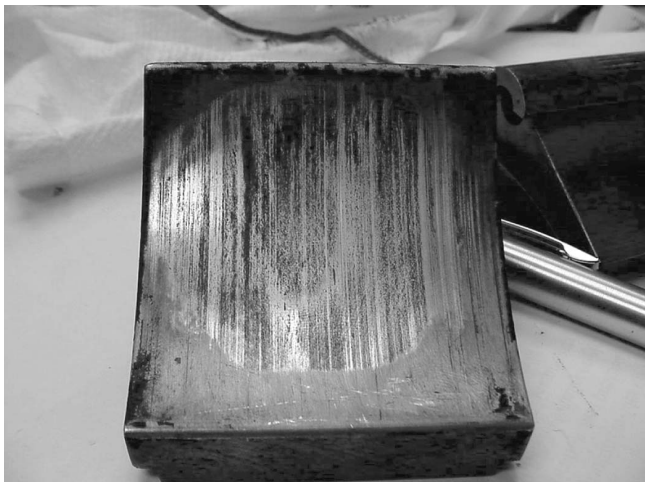

Figure 42. One of Lower NDE Bearings with Varnish Buildup (Babbitt is Not *Wiped).*

Figure 43. One of the Lower NDE Bearing Pads Showing Dimple Where Babbitt Failed above RTD.

determine the source of the vibration. Figure 47 shows the radial vibration on a centrifugal compressor while the speed was increased from 11,000 to 12,200 rpm. As can be seen, the vibration increased from approximately 1.4 mils peak-to-peak to over 3 mils

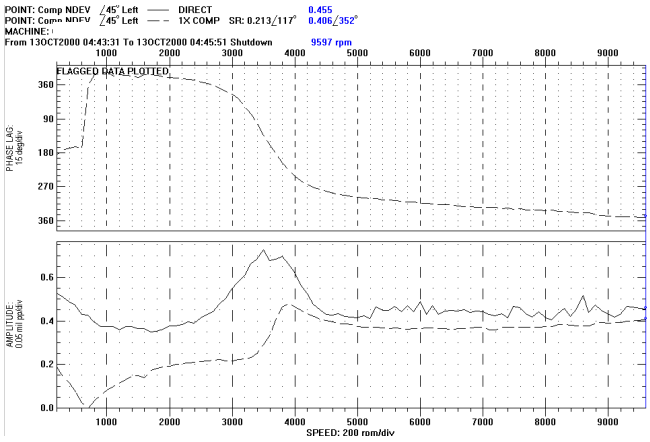

Figure 44. Startup Bodé Plot of Centrifugal Compressor after Oil Obstruction Was Removed.

peak-to-peak. Examination of the orbits before and during the speed change showed two large internal loops appear at the higher speed (Figures 46 and 48). This is indicative of a subsynchronous frequency at approximately one-third of running speed (Equation (4).

$$Vib\ Frequency = \frac{shaft\ speed}{\#\ of\ \text{int}ernal\ loops + 1} \tag{4}$$

A rotordynamic analysis of the compressor revealed that the first mode (at one-third of running speed) was only marginally stable. Additionally, changes in alignment or preload can cause strange looking orbits. Figure 49 shows how preload in one direction affects the orbit shape. Figure 50 shows the orbit from an induction motor that has severe temperature related vibration problems. The overall vibration amplitude would reach 8 mils on this particular machine during the heat of the summer and drop to 2 mils during the winter.

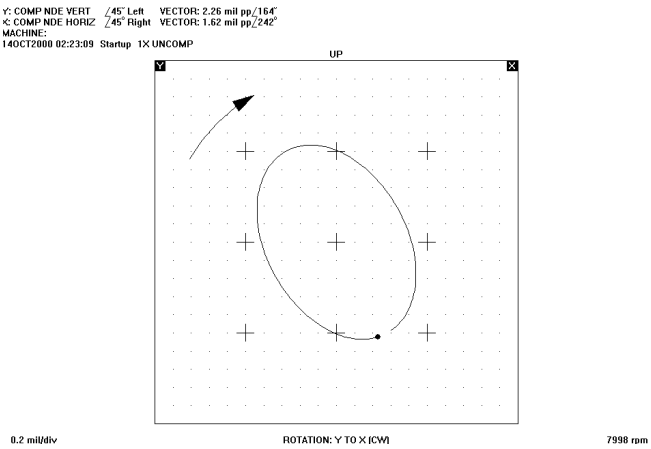

Figure 45. Shaft Orbit.

USING STARTUP/SHUTDOWN DATA IN CONJUNCTION WITH ROTORDYNAMIC MODELS

Startup/shutdown data can be used as a very important tool to validate and/or tune rotordynamic models of turbomachinery. While the accuracy of rotordynamic models has increased, actual measured critical speeds and amplitudes are still very important in evaluating a machine's condition. Additionally, rotordynamic models can be used to gain insight into some startup and shutdown data.

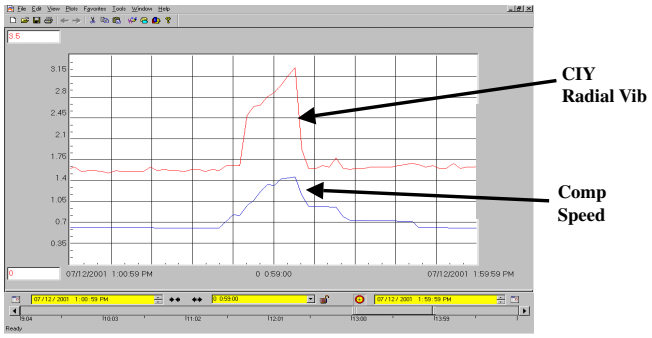

Figure 46. Large Increase in Radial Vibration during Speed Change.

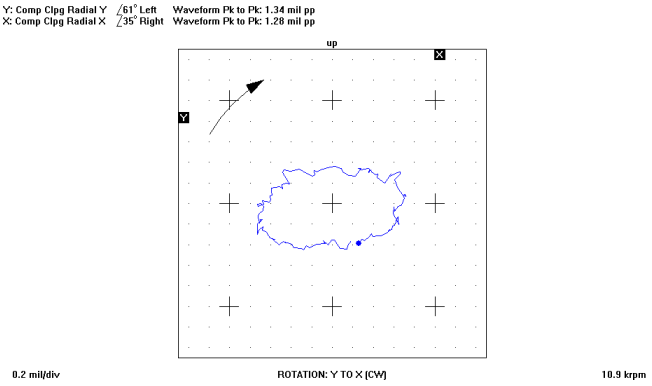

Figure 47. Orbit at 11,000 RPM.

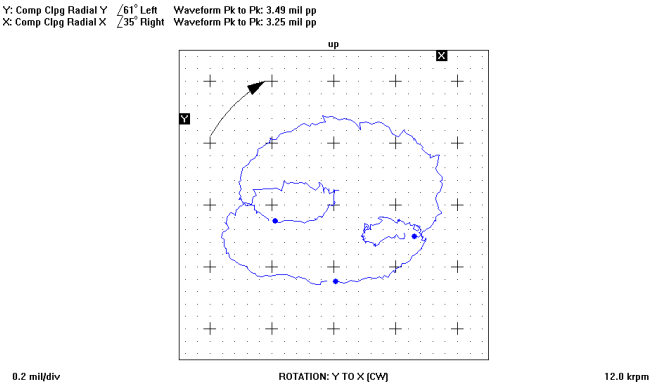

Figure 48. Orbit Showing Subsynchronous Component at 12,000 RPM.

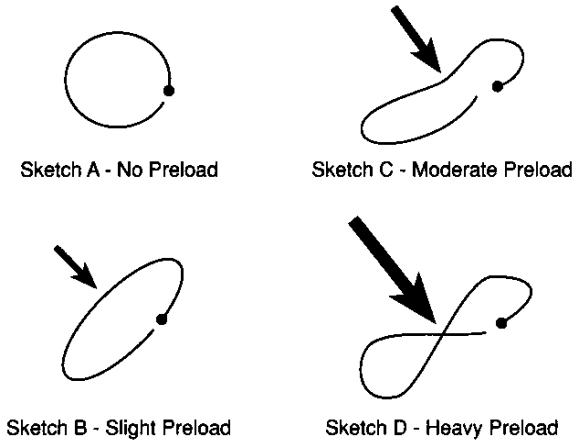

Figure 49. Change in Shaft Orbits with Increasing Preload.

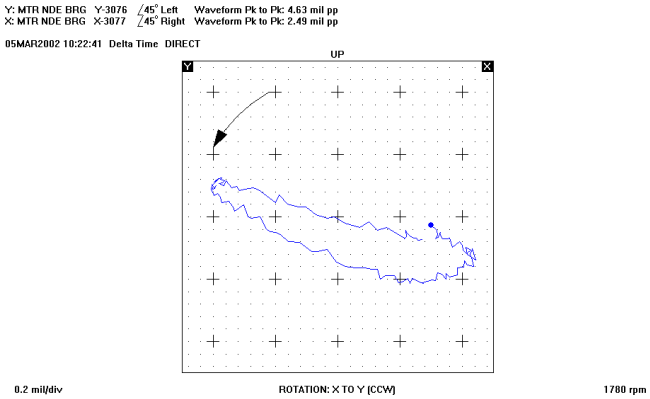

Figure 50. Induction Motor with Severe Internal Misalignment.

Case Study 5—High Synchronous Vibration on Centrifugal Compressor after Rerate

A small high-speed, multistage barrel compressor was rerated because the molecular weight of the gas was lower than the original design. This required that the speed be increased from 17,500 to 19,500 rpm. Because the compressor would be operating closer to its second critical speed, the spare rotor was at-speed balanced. The rerated rotor was installed and the compressor was restarted. The synchronous radial vibration on the nondrive-end of the compressor was approximately 1.5 mils. While 1.5 mils is not normally considered excessive for lower speed machines, at 19,500 cpm this is much too high. The startup Bodé plots for the drive-end and nondrive-end are shown in Figure 51. Note the differences in shape between the drive- and nondrive-end plots. Comparison to the predicted response for the minimum and maximum bearing and seal clearance in Figures 52 and 53 indicates that the high synchronous vibration is probably caused by higher clearances instead of imbalance. Additionally, examination of the orbits from both bearings shows a lubricated rub on the drive-end (Figures 54 and 55). Note that the orbit with the inner loops is on the drive-end (which has the lower vibration). Examination of the repair records showed that the bearing and seal clearances on the nondrive-end were at the maximum of the allowable clearance.

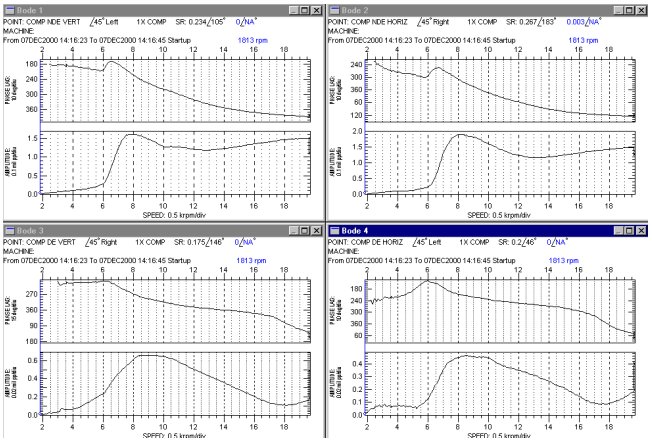

Figure 51. Bodé Plots of High-Speed Centrifugal Compressors with Excessive Synchronous Vibration after At-Speed Balance.

SUMMARY

Transient vibration data provide a wealth of information about the condition of the machinery that is not available from steady-state data. Likewise, all the different transient plot types must be used to get the most from the data. This information can be used to evaluate the condition of the bearings as well as help determine the

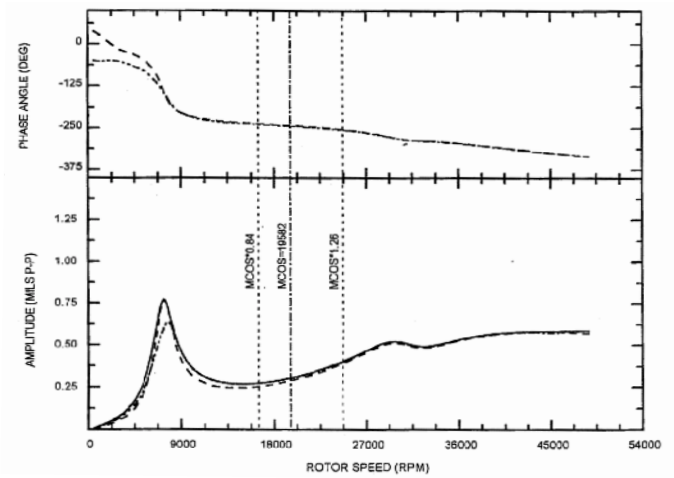

Figure 52. Predicted Unbalance Response with Nominal Bearing and Seal Clearances.

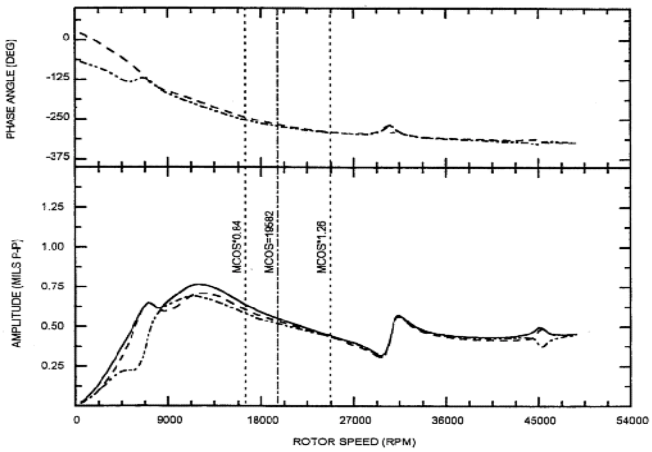

Figure 53. Predicted Unbalance Response with Maximum Bearing and Seal Clearances.

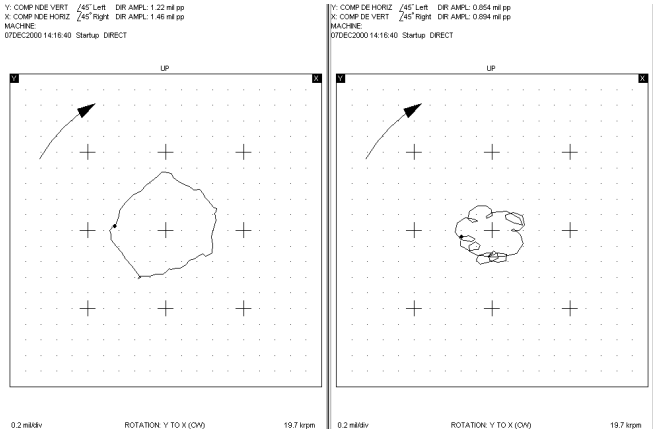

Figure 54. Orbits of NDE and DE of High-Speed Centrifugal Compressor.

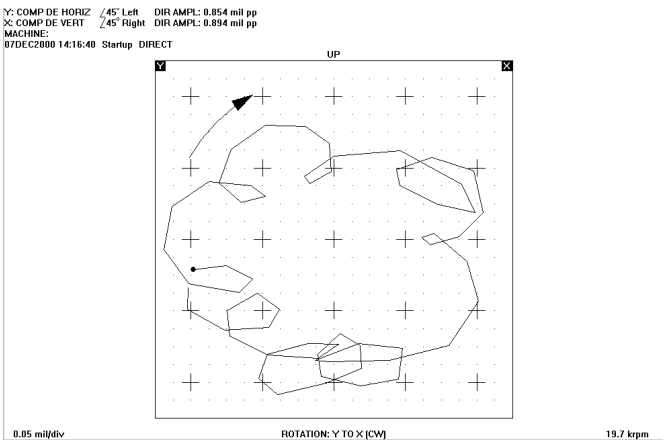

Figure 55. Closeup of DE Orbit on High-Speed Centrifugal Compressor Showing Lubricated Rub.

cause of excitation forces such as unbalance and rubs when it is not immediately obvious. Transient data also provide a method of verifying machinery natural mode frequencies and rotordynamic models.

ACKNOWLEDGEMENTS

This paper would not have been possible without the gifts given the author by his Lord and Savior Jesus Christ. Additionally, the author will always be in debt to his wife, Angie, and his four daughters, Lauren, Bailey, Allie, and Peyton, for their patience in letting him take the time to write this paper. The author would also like to thank Charlie Jackson and Charlie Rutan for providing some of the figures in this paper.

REFERENCES

Barrett, L. E., Gunter, E. J., and Allaire, P. E., 1978, "Optimum Bearing Support Damping for Unbalance Response and Stability of Rotating Machinery," *Journal of Engineering for Power*, *100*, pp. 89-94.

Bielk, J. R. and Leader, M. E., 1994, "Rotordynamics," Short Course 2, Twenty-Third Turbomachinery Symposium, Turbomachinery Laboratory, Texas A&M University, College Station, Texas.

Eisenmann, R. C. and Eisenmann Jr., R. C., 1998, *Machinery Malfunction Diagnosis and Correction*, New Jersey: Prentice Hall.

Vance, J., 1988, *Rotordynamics of Turbomachinery*, New York, New York: John Wiley.

Zeidan, F. Y. and Herbage, B. S., 1991, "Fluid Film Bearing Fundamentals and Failure Analysis," *Proceedings of the Twentieth Turbomachinery Symposium*, Turbomachinery Laboratory, Texas A&M University, College Station, Texas, pp. 161-186.

BIBLIOGRAPHY

Childs, D. W., 1993, *Turbomachinery Rotordynamics*, New York, New York: John Wiley.